

Enacyloxins Are Products of an Unusual Hybrid Modular Polyketide Synthase Encoded by a Cryptic *Burkholderia ambifaria* Genomic Island

Eshwar Mahenthiralingam,^{1,*} Lijiang Song,² Andrea Sass,¹ Judith White,¹ Ceri Wilmot,¹ Angela Marchbank,¹ Othman Boaisa,¹ James Paine,³ David Knight,³ and Gregory L. Challis^{2,*}

¹Organisms and Environment Division, Cardiff School of Biosciences, Cardiff University, Main Building, Park Place, Cardiff, Wales CF10 3AT, UK

²Department of Chemistry, University of Warwick, Coventry, West Midlands, England CV4 7AL, UK

³School of Chemistry, Cardiff University, Main Building, Park Place, Cardiff, Wales CF10 3AT, UK

*Correspondence: mahenthiralingame@cardiff.ac.uk (E.M.), g.l.challis@warwick.ac.uk (G.L.C.)

DOI 10.1016/j.chembiol.2011.01.020

SUMMARY

Gram-negative *Burkholderia cepacia* complex (Bcc) isolates were screened for antimicrobial activity against cystic fibrosis microbial pathogens, and the ability of *B. ambifaria* to inhibit *B. multivorans* was identified. The activity was mapped to a cluster of cryptic, quorum-sensing-regulated modular polyketide synthase (PKS) genes. Enacyloxin IIa and its stereoisomer designated *iso*-enacyloxin IIa were identified as metabolic products of the gene cluster, which encoded an unusual hybrid modular PKS consisting of multiple proteins with sequence similarity to *cis*-acyltransferase (*cis*-AT) PKSs and a single protein with sequence similarity to *trans*-AT PKSs. The discovery of the potent activity of enacyloxins against drug-resistant bacteria and the gene cluster that directs their production provides an opportunity for engineered biosynthesis of innovative enacyloxin derivatives and highlights the potential of Bcc bacteria as an underexploited resource for antibiotic discovery.

INTRODUCTION

Bacteria within the Gram-negative genus *Burkholderia* are well known for their phenotypic and genotypic diversity (Coenye and Vandamme, 2003). The *Burkholderia cepacia* complex (Bcc) is a subgroup of closely related *Burkholderia* species that reflect this functional multiplicity by demonstrating biopesticidal interactions at the plant rhizosphere (Parke and Gurian-Sherman, 2001), a capacity for the bioremediation of aromatic hydrocarbon pollutants (Chain et al., 2006; O'Sullivan et al., 2007), and also the ability to cause devastating lung infections in individuals with cystic fibrosis (CF) (Mahenthiralingam et al., 2005). The taxonomy of *B. cepacia* complex isolates has undergone extensive revision over the last decade, with expansion from 1 to 17 formally named Bcc species (Mahenthiralingam et al., 2008; Vanlaere et al., 2009). All Bcc bacteria possess intrinsic resistance to a range of antimicrobial compounds

including antibiotics and biocides (Rose et al., 2009), and infections in patients with CF are difficult to treat with currently available antibiotics (Chernish and Aaron, 2003). Outside of CF infection, the rhizosphere is the best-characterized environmental habitat of Bcc bacteria (Parke and Gurian-Sherman, 2001), where their biopesticidal ability to protect crops from fungal and nematodal pathogens has been linked in part to their ability to biosynthesize a range of antibiotic or toxic secondary metabolites (Parke and Gurian-Sherman, 2001; Vial et al., 2007).

Antifungal antibiotics known to be produced by Bcc species include cepacin, cepaciamide, xylocandins, quinolinones, phenylpyrroles, and phenazines (Parke and Gurian-Sherman, 2001; Vial et al., 2007). An antifungal nonribosomally biosynthesized lipopeptide, AFC-BC11, has been genetically characterized in *B. cepacia* strain BC11 (Kang et al., 1998), and the recently described Burkholdines 1097 and 1229 are antifungal cyclic lipopeptides produced by *B. ambifaria* 2.2N (Tawfik et al., 2010). One of the most well known Bcc antibiotics is pyrrolnitrin, a broad-range antifungal phenylpyrrole that has been recently found to be produced by several Bcc species under the control of quorum sensing (QS) (Schmidt et al., 2009). *Burkholderia* secondary metabolites may also have multiple functions, such as the 4-quinolinones which were originally characterized as antifungal antibiotics and plant growth-promoting agents (Moon et al., 1996), and more recently derivatives such as 2-heptyl-3-hydroxy-4(1*H*)-quinolone have also been shown to act as a quorum-sensing signal in *B. ambifaria* and other non-Bcc *Burkholderia* species (Diggle et al., 2006; Vial et al., 2008). Several studies have demonstrated that non-Bcc *Burkholderia* species are capable of producing polyketide antibiotics such as the rhizoxin toxin which causes rice blight (Partida-Martinez and Hertweck, 2007), the bactobolins which have antibacterial activity (Seyedsayamdost et al., 2010), and the food-related toxin bronkrecic acid (Rohm et al., 2010). In addition to the identification of antimicrobials naturally produced by *Burkholderia* bacteria, Knappe et al. (2008) used a genome-mining approach to isolate capistruiin, a lasso peptide encoded by the *B. thailandensis* genome. Bioinformatic analysis of the ketosynthase (KS) domains of *trans*-acyltransferase (AT) polyketide synthase (PKS)-encoding genes also enabled the identification of thailandamide polyketides within the *B. thailandensis* genome and their subsequent biological analysis (Nguyen et al., 2008).

Given the extent to which the taxonomic description of Bcc species has changed and the limited number of antibiotics characterized in well-defined *Burkholderia* species (Schmidt et al., 2009; Seyedsayamdost et al., 2010; Tawfik et al., 2010; Vial et al., 2007), we performed a systematic survey of antimicrobial activity across a large collection of genetically typed Bcc strains. In addition, because it has been anecdotally observed that CF sputum appears less polymicrobial once chronic infection with a Bcc isolate is established, we also specifically screened for Bcc antagonism toward other CF pathogens such as *Pseudomonas aeruginosa*, *Staphylococcus aureus*, the yeast *Candida albicans*, as well as other Bcc species (Lipuma, 2010). A broad range of antimicrobial Bcc phenotypes was observed, the most remarkable of which was the activity against multidrug-resistant (MDR) Gram-negative bacteria shown by *B. ambifaria*, a species previously known for its antifungal and biopesticidal properties (Coenye et al., 2001). Using transposon mutagenesis, we mapped the genes responsible for the antibacterial activity to a putative polyketide biosynthesis island within the genome of *B. ambifaria* AMMD, and together with global gene expression identified multiple accessory loci required for antibiotic biosynthesis. Purification and spectroscopic analysis of the compounds responsible for the anti-Gram-negative activity identified them as enacyloxins (Watanabe et al., 1982), unusual polyene antibiotics that target protein biosynthesis by inhibition of the ribosomal elongation factor Tu (Parmeggiani et al., 2006). LC-MS analyses confirmed that enacyloxin production was abolished in the transposon mutants. Sequence comparisons of the enzymes encoded by genes within the enacyloxin biosynthetic gene cluster suggest a complete hypothetical pathway for enacyloxin biosynthesis involving an extremely unusual hybrid PKS composed of proteins with sequence similarity to both the phylogenetically distinct *cis*-AT and *trans*-AT PKS families (Piel, 2010), several PKS modules with sequence similarity to *cis*-AT proteins that lack AT domains, a unique mechanism for polyketide chain release, and both nonheme iron- and flavin adenine dinucleotide (FAD)-dependent chlorinases. The enacyloxins appear to be one of an armory of antimicrobial compounds synthesized by *B. ambifaria*, and the mapping of their biosynthetic pathway reflects the remarkable diversity of antimicrobial functions that can be acquired and expressed by these versatile bacteria.

RESULTS

Prevalence of Antimicrobial Activity within the Bcc

An initial screen for antimicrobial activity was performed on nine genome-sequenced Bcc strains and nine other representative isolates (see Experimental Procedures). To stimulate secondary metabolite production, Bcc bacteria were (1) grown on a minimal medium containing glycerol, a carbon source that often promotes antibiotic production (Keum et al., 2009); (2) incubated for 5 days such that stationary phase was reached; and (3) grown as a dense single colony where biofilm- and quorum-sensing interactions could promote alternative metabolism and catabolism (see Experimental Procedures). After growth, the Bcc strains were overlaid with *B. multivorans* and a zone of clearing was observed around the *B. ambifaria* AMMD colony (Figure 1A). The demonstration of novel anti-Gram-negative

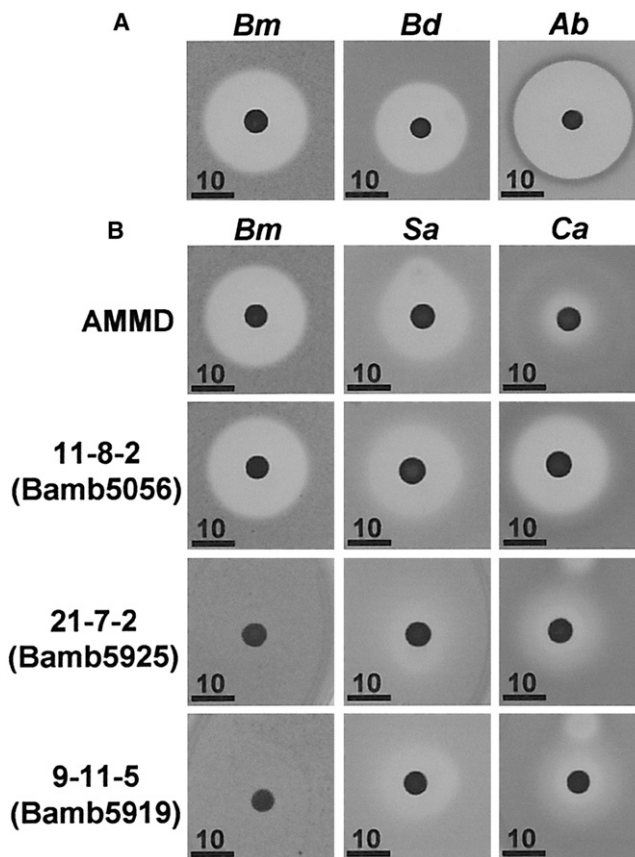


Figure 1. The Novel Anti-Gram-Negative Activity of *B. ambifaria*

The results of a *B. ambifaria* strain AMMD antimicrobial screening assay are shown for overlays with three multidrug-resistant bacteria in (A): *Bm*, *B. multivorans* C1576 (Glasgow outbreak strain); *Bd*, *B. dolosa* LMG 18943 (Boston outbreak strain); and *Ab*, *A. baumannii* OXA23 clone 2. The antimicrobial phenotypes of wild-type *B. ambifaria* strain AMMD, a rapid secretor mutant (11-8-2), and two PKS mutants within the biosynthesis island (21-7-2 and 9-11-5) are shown against overlays of *B. multivorans* (*Bm*), *S. aureus* (*Sa*), and *C. albicans* (*Ca*) in (B). The gene inactivated by the transposon insertion is shown in brackets (see Table 2). The figure comprises a composite of proportionately cropped images of overlay assays, and a scale bar of 10 mm is shown in each panel to indicate the size of the zone of antimicrobial inhibition. See also Figures S1 and S2.

activity in *B. ambifaria* was expanded to a systematic screen of 268 Bcc isolates, comprising 13 named species and 5 novel subgroups within the complex (Table 1); 228 of these isolates were genetically distinct strains by multilocus sequence typing (MLST) (Baldwin et al., 2005), and the collection possessed a similar number of isolates from clinical infections (43%) and from the natural environment (57%). Antimicrobial activity against a panel of CF pathogens including Gram-negative bacteria (*P. aeruginosa* and *B. multivorans*), Gram-positive bacteria (*S. aureus*), and fungi (*C. albicans*) was examined (Table 1).

No antagonism toward *P. aeruginosa* was observed; however, 32% of the Bcc isolates demonstrated anticandidal properties and 24% were capable of inhibiting the growth of *S. aureus* (Table 1). *B. cepacia*, *B. cenocepacia*, *B. stabiliz*, *B. vietnamiensis*, and *B. ambifaria* were active against *S. aureus*,

Table 1. Collection of *B. cepacia* Complex Isolates Screened for Antimicrobial Activity

Species or Bcc Subgroup	Number of Isolates (Clinical/Environmental)	Number of Strains (Based on MLST Sequence Types)	Number with Antimicrobial Activity ^a (% Isolates within Each Bcc Species)		
			<i>B. multivorans</i>	<i>S. aureus</i>	<i>C. albicans</i>
<i>B. cepacia</i>	30 (15/15)	29	0	11 (37)	14 (47)
<i>B. multivorans</i>	24 (20/4)	24	0	0	0
<i>B. cenocepacia</i> III-A	28 (25/3)	22	0	8 (29)	1 (4)
<i>B. cenocepacia</i> III-B	30 (11/19)	27	0	9 (30)	7 (23)
<i>B. stabilis</i>	16 (10/6)	7	0	9 (56)	0
<i>B. vietnamiensis</i>	16 (5/11)	12	0	7 (44)	7 (44)
<i>B. dolosa</i>	8 (8/0)	5	0	0	0
<i>B. ambifaria</i>	46 (6/40)	43	6 (13)	17 (37)	21 (46)
<i>B. anthina</i>	14 (4/10)	9	0	1 (7)	6 (43)
<i>B. pyrrocinia</i>	16 (2/14)	13	0	1 (6)	9 (56)
<i>B. arboris</i>	3 (1/2)	3	0	0	0
<i>B. diffusa</i>	1 (0/1)	1	0	0	0
<i>B. lata</i>	10 (1/9)	8	0	1 (10)	4 (40)
<i>B. contaminans</i>	6 (4/2)	6	0	0	3 (50)
Bcc group K (novel)	1 (0/1)	1	0	0	0
BCC4	3 (1/2)	3	0	0	3 (100)
BCC5	5 (2/3)	5	0	0	3 (60)
BCC6	10 (0/10)	9	0	0	7 (70)
BCC8	1 (1/0)	1	0	0	0
Total	268 (116/152)	228	6 (2.2)	64 (24)	85 (32)

^aA zone of clearing ≥ 10 mm was scored as positive for antimicrobial activity.

with greater than 29% of isolates in each species producing inhibition zones; the same Bcc species were also highly antagonistic toward *C. albicans* (Table 1). Antifungal activity was also seen in *B. anthina*, *B. pyrrocinia*, *B. arboris*, *B. lata*, *B. contaminans*, and several of the novel Bcc MLST groups (Table 1). No antagonistic activity was observed for any *B. multivorans*, *B. stabilis*, *B. dolosa*, *B. arboris*, or *B. diffusa* isolates tested (Table 1). Anti-Gram-negative activity was not common in the Bcc (Table 1); however, six *B. ambifaria* isolates strongly inhibited the growth of *B. multivorans* (Figure 1), and the genome-sequenced species-type strain for *B. ambifaria*, strain AMMD (Coenye et al., 2001) (see <http://www.burkholderia.com>) was selected for further study of this novel activity.

***B. ambifaria* Produces an Antimicrobial Active on Other Bcc Bacteria**

B. ambifaria AMMD inhibited the growth of all *B. multivorans* ($n = 11$) and *B. dolosa* ($n = 7$) strains tested. Notably, the AMMD antimicrobial was also active against pan-resistant Gram-negative strains such as the *B. multivorans* Glasgow CF strain (Rose et al., 2009), *B. dolosa* Boston CF strain (Kalish et al., 2006), and *Acinetobacter baumannii* OXA23 clone 2 (Coelho et al., 2006) (Figure 1A). *B. cepacia*, *B. cenocepacia*, *B. stabilis*, *B. vietnamiensis*, *B. ambifaria*, *B. lata*, and *B. diffusa* were all resistant to the *B. ambifaria* AMMD antimicrobial; both susceptible and resistant strains were found among the *B. vietnamiensis*, *B. pyrrocinia*, and *B. anthina* strains examined. The unique anti-Gram-negative activity of *B. ambifaria* was designated "*B. ambifaria* antimicrobial on *B. multivorans*"

(BAMM). Secretion of BAMM was not constitutive and remained cryptic unless it was induced by growth on carbon sources such as glycerol and ribose and the cultures allowed to reach stationary phase (approximately 30 hr at 30°C).

The Genetic Basis of *B. ambifaria* Anti-Gram-Negative Activity

Transposon mutagenesis (O'Sullivan et al., 2007) was used to identify genes required for the biosynthesis of BAMM in *B. ambifaria* AMMD. Of 1920 mutants screened, 22 with an altered BAMM phenotype (Figure 1B) were identified and mapped to the AMMD genome (Table 2). Four transposon insertions mapped to chromosome 1 (Table 2): mutations within general secretory pathway genes either stopped BAMM production or reduced it; mutation of a type I glycosyltransferase within an exopolysaccharide gene cluster gave a BAMM-negative phenotype; and transposon insertion into an AraC-type transcriptional regulator coding sequence (CDS) resulted in early onset of BAMM secretion (a zone of clearing was seen after 18 hr). The same rapid secretion phenotype was seen with mutation of a cation diffusion facilitator family transporter gene (Bamb_5056, mutant 11-8-2) encoded on chromosome 2 (Table 2), which also demonstrated greater anticandidal activity than the wild-type (Figure 1B). Five independently isolated BAMM-negative mutants mapped to the same locus on chromosome 2, a hypothetical gene, Bamb_5367, adjacent to a recombination hot spot (RHS) element, Bamb_5366, encoding a valine-glycine-rich protein (VGR) protein. Another interesting chromosome 2 mutation which stopped BAMM secretion was

Table 2. Transposon Mutants of *B. ambifaria* AMMD with Altered BAMB Properties

Mutant Name (Chromosomal Location)	BAMB Phenotype	Gene	Putative Function	Microarray Expression Analysis ^a	
				Fold Change	p Value
Chromosome 1					
4-11-5	Negative	Bamb_0051	General secretory pathway protein E	2.354	0.00412
3-12-1	Weak ^b	Bamb_0052	General secretory pathway protein D	2.415	0.00571
5-5-3	Negative	Bamb_0758	Glycosyltransferase, group 1	6.581	0.00844
5-3-7	Rapid ^c	Bamb_2222	Transcriptional regulator, AraC family	-	-
Chromosome 2					
5-7-2	Negative	Bamb_4118	Autoinducer synthase, CepsI	-2.183	0.0469
9-7-2	Negative	Bamb_4118	Autoinducer synthase, CepsI	-2.183	0.0469
11-8-2	Rapid ^c	Bamb_5056	Cation diffusion facilitator family transporter	-	-
10-11-3	Negative	Bamb_5367	Hypothetical protein	-	-
8-7-6	Negative	Bamb_5367	Hypothetical protein	-	-
11-10-3	Negative	Bamb_5367	Hypothetical protein	-	-
13-12-6	Negative	Bamb_5367	Hypothetical protein	-	-
1-9-5	Negative	Bamb_5367	Hypothetical protein	-	-
Chromosome 3					
20-11-1	Negative	Bamb_5910	Transcriptional regulator, LuxR family	4.079	0.00071
9-11-5	Negative	Bamb_5919	<i>trans</i> -AT modular PKS	92.17	0.00172
18-3-4	Negative	Bamb_5921	<i>cis</i> -AT modular PKS	72.21	0.00049
16-6-5	Negative	Bamb_5921	<i>cis</i> -AT modular PKS	72.21	0.00049
15-4-3	Negative	Bamb_5924	<i>cis</i> -AT modular PKS	8.829	0.00209
9-3-8	Negative	Intergenic Bamb_5924–5925	<i>cis</i> -AT modular PKS	-	-
21-7-2	Negative	Bamb_5925	<i>cis</i> -AT modular PKS	159.5	0.00119
19-11-4	Negative	Bamb_5926	Type II thioesterase	1.89	0.00903
20-6-6	Negative	Bamb_5928	FADH ₂ -dependent chlorinase	292.7	0.00176
2-6-7	Negative	Bamb_6239	UDP-glucuronosyl/UDP-glucosyltransferase	-	-

See also Table S4.

^a Further information on the alterations in gene expression observed during antibiotic production are shown in Table S4 and Supplemental Information file *B_ambifaria_genes_induced_by_glycerol.xls*.

^b Weak zone of clearing <10 mm observed around the *B. ambifaria* AMMD mutant.

^c Secretion of BAMB appeared after 18 hr of growth as indicated by a small but clear zone of clearing >10 mm.

that of Bamb_4118 (two independent mutants; Table 2), a homolog of the acyl homoserine lactone (AHL) synthase, CepsI, associated with Gram-negative QS systems (Malott et al., 2005). The lack of BAMB secretion in the *cepsI* mutant suggested that QS plays an integral role in activating antibiotic biosynthesis correlating to the stationary phase growth onset of BAMB secretion.

Nine mutants mapped to the same region on chromosome 3, a large genomic island (87.4 kb; coordinates 392535–479734) with a 71.5% GC content compared to the 66.5% GC average for this *B. ambifaria* AMMD replicon. The island spanned 33 coding sequences (Bamb_5910–5943; see Table S1 available online for function and homology data). Several CDSs encoded proteins with similarity to known modular PKSs, suggesting the BAMB antimicrobial was a polyketide (Nguyen et al., 2008; Zerikly and Challis, 2009). The organization of the 24 genes within the island is shown in Figure 2. Transposon mutations resulting in a BAMB-negative phenotype were mapped to four of the seven PKS CDSs (Figure 2 and Table 2). Transposon insertions mapped to a type II thioesterase (proposed in other

systems to maintain PKS activity by catalyzing hydrolysis of aberrant intermediates that block procession of the growing polyketide chain along the PKS), and FADH₂-dependent chlorinase upstream of these genes also abrogated BAMB production (Table 2 and Figure 2). Downstream of the PKS genes and at the far end of the genomic island were two genes encoding putative LuxR-type regulators, one of which, Bamb_5910, was mapped by a transposon insertion which resulted in a BAMB-negative phenotype. Because mutation of the Bamb_4118 AHL synthase had also prevented BAMB secretion, it was not surprising to find that mutation of a LuxR regulator within the island stopped production of the antimicrobial.

Transposon inactivation of the PKS genes (Figure 2) resulted in mutants that produce no zones of inhibition in the *B. multivorans* overlay assays (data shown for the Bamb_5925 and Bamb_5919 mutants, 21-7-2 and 9-11-5, respectively, in Figure 1B). These PKS mutants still produced a zone of inhibition against *S. aureus*, although the activity was weaker than the wild-type (Figure 1B). Interestingly, the anticandidal activity of *B. ambifaria* AMMD was unaffected by mutation of the PKS genes (Figure 1B), suggesting

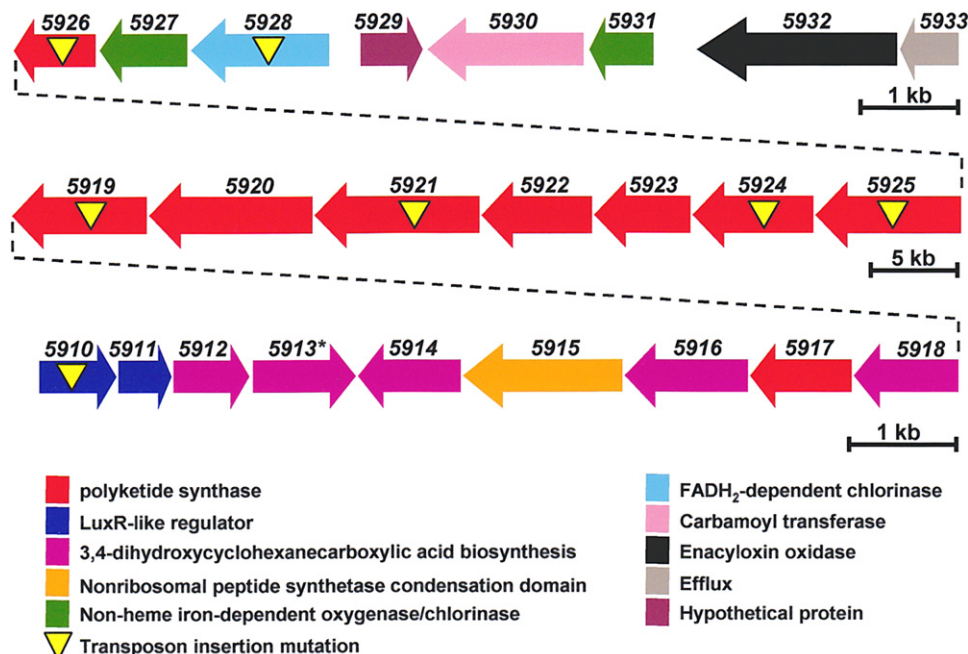


Figure 2. Genetic Organization of the *B. ambifaria* AMMD Polyketide Biosynthesis Island

The arrangement of 24 genes within the polyketide biosynthesis island is shown as three panels, each drawn to the scale given by the bars on the right of each respective panel. The functional contribution of each gene to polyketide biosynthesis is shown by the color-coded key, and genes mapped by transposon mutagenesis (see Table 2) are indicated. All genes in the pathway shown above were significantly upregulated under antibiotic-inducing growth conditions (see Table S4) except Bamb_5913 (*). Homology data to support the putative function of each gene are provided in Table S1, with the microarray demonstrating upregulation of the gene cluster during enacyloxin production-inducing growth conditions provided in Table S4.

that the polyketide antibiotic being produced from the PKS cluster had limited antifungal activity as detected by the colony overlay assay. None of the transposon mutants demonstrated increased susceptibility to the AMMD polyketide when they were themselves overlaid onto a wild-type *B. ambifaria* AMMD colony, indicating that the genes identified as essential for BAMB production (Table 2) did not play a role in self-resistance to the secreted antimicrobial. PCR primers designed to detect three PKS-encoding genes, Bamb_5925, Bamb_5921, and Bamb_5919 (Figure 2), amplified the corresponding loci from five other *B. ambifaria* strains (BCC0118, BCC0203, BCC0250, BCC0480, and BCC1254) that also demonstrated BAMB activity (Table 1). The positive bioactivity and presence of homologous genes spanning the PKS region suggested that all these *B. ambifaria* isolates possessed a functional BAMB polyketide biosynthesis island even though each was a genetically distinct strain by MLST.

Isolation and Structure Elucidation of the Metabolic Product of the Cryptic BAMB Polyketide Biosynthetic Gene Cluster

Adsorption of the presumed polyketide product of the conserved genomic island onto XAD-16, a neutral crosslinked polystyrene resin that adsorbs erythromycin from solution (Ribeiro and Ribeiro, 2003), was investigated as an initial step in the isolation of the BAMB activity. Active methanol eluates were obtained from adsorption of the supernatants of liquid cultures and aqueous washes of the agar from solid-medium growth of

B. ambifaria AMMD (see Experimental Procedures). The eluates obtained from agar-grown bacteria proved most stable, and LC-MS analysis indicated that they contained several compounds. The eluates were therefore further fractionated by semipreparative HPLC, and each fraction was analyzed by high-resolution electrospray ionization mass spectrometry (HR-ESI-MS).

One fraction afforded ions with $m/z = 256.1694$ and 258.1848 (Figure S1). The molecular formulas deduced for these ions (calculated for $C_{17}H_{22}NO^+$: 256.1696, and for $C_{17}H_{24}NO^+$: 258.1852) correspond to 2-(2-heptenyl)-3-methyl-4-quinolinone and 2-heptanyl-3-methyl-4-quinolinone, respectively (Figure S1), known antifungal agents originally isolated from “*Pseudomonas cepacia*” strain PCII (Moon et al., 1996) (the taxonomic status of this Bcc isolate is not known). MS/MS analyses indicated that these compounds contain a common 3-methyl-4-quinoline core and a heptenyl/heptyl side chain, respectively (Vial et al., 2008). *B. ambifaria* has previously been reported to produce these molecules as quorum-sensing signals (Vial et al., 2008), suggesting that these *Burkholderia* secondary metabolites may play multiple roles. The *B. ambifaria* AMMD genome contains a corresponding 2-alkyl-3-methyl-4-quinolinone biosynthetic gene cluster, *hmqA-G* (Bamb_5763–5769), on chromosome 3 approximately 166 kb downstream of the BAMB polyketide biosynthesis island.

Another fraction afforded an ion with $m/z = 702.2446$. This corresponds to the molecular formula of the known polyketide antibiotic enacyloxin IIa (calculated for $C_{33}H_{46}NO_{11}Cl_2^+$: 702.2442) (Watanabe et al., 1992). This fraction also had an

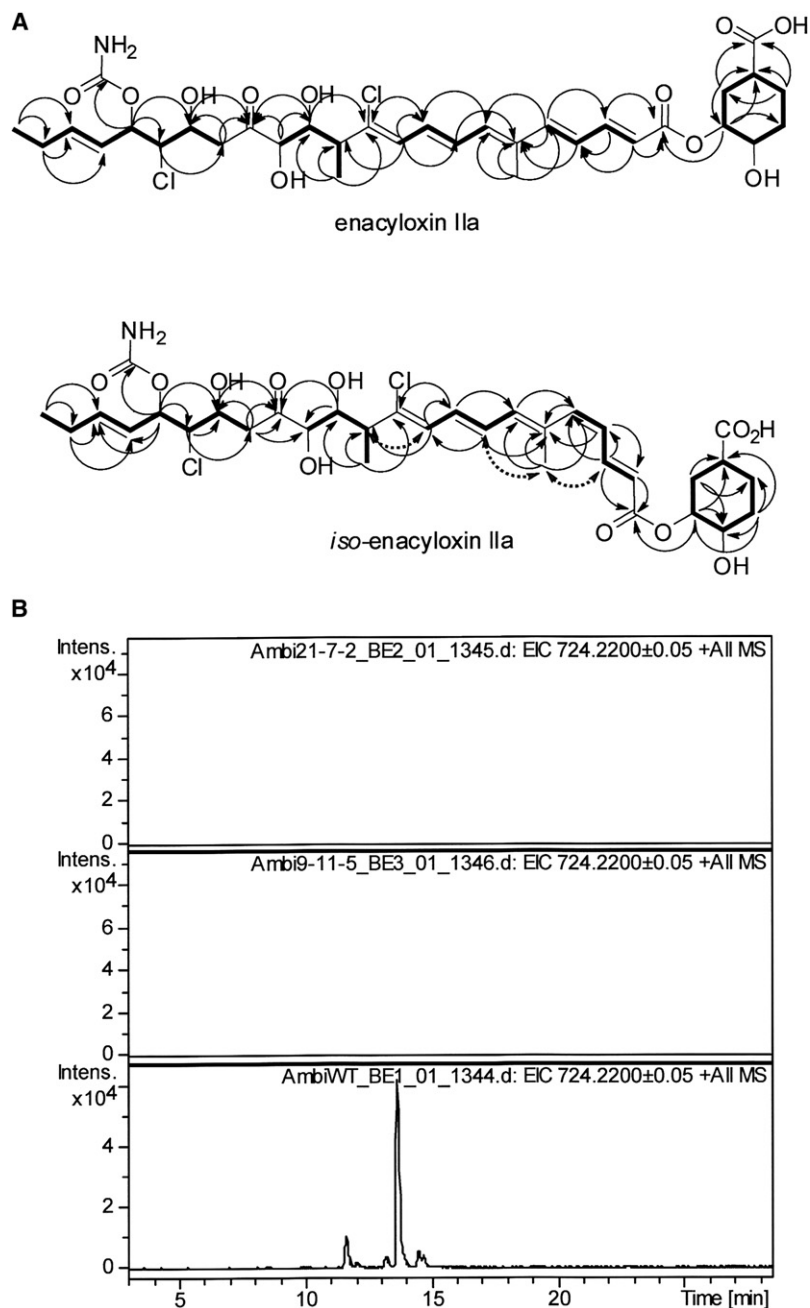


Figure 3. Structures of Enacyloxin IIa and iso-Enacyloxin IIa

(A) A summary of COSY (bold lines), HMBC (black arrows), and NOESY (dashed arrows) correlations observed for enacyloxin IIa and iso-enacyloxin IIa.

(B) LC-MS analysis and extracted ion chromatograms (M+Na) at m/z 724.2200 \pm 0.05 for the *B. ambifaria* AMMD amberlite resin eluates of the PKS mutants 21-7-2 (top) and 9-11-5 (middle) and the wild-type strain (bottom); enacyloxin IIa and iso-enacyloxin signals are absent from the PKS mutants, linking the pathway to production of the antibiotics. Data to support the assigned structure are provided in Tables S2 and S3.

cryptic PKS gene cluster (21-7-2, Bamb_5925 and 9-11-5, Bamb_5919; Figures 1B and 2) indicated that they did not contain enacyloxins (Figure 3), unequivocally linking enacyloxin biosynthesis to this novel biosynthetic island. The 4-quinolinone metabolites (Figure S1) could still be detected by LC-MS in the XAD-16 eluates of the mutants, correlating with the retained anticandidal properties of the mutants (Figure 1B).

Antimicrobial Spectrum of the *B. ambifaria* Enacyloxins

Antibiotic susceptibility testing (Table 3) was performed on enacyloxin IIa and iso-enacyloxin IIa purified from *B. ambifaria*. These experiments demonstrated that both had novel and highly potent activity against *B. multivorans*, *B. dolosa*, and *A. baumannii*, all of which are considered pan-resistant Gram-negative pathogens. Enacyloxin IIa was approximately twice as active as iso-enacyloxin IIa (Table 3), suggesting that the change in the configuration of the 4,5-double bond in iso-enacyloxin IIa either reduces its ability to penetrate these pathogens or, more likely, alters its ability to bind to its target, the elongation factor Tu (Parmeggiani et al., 2006). *P. aeruginosa* and *B. cenocepacia* were both resistant to the maximum concentration tested (100 mg/l). The purified enacyloxins also lacked inhibitory activity against *C. albicans* at 100 mg/l, correlating with the observation that the PKS

absorbance maximum at 360 nm in the UV/vis spectrum, consistent with the polyene chromophore of the enacyloxins. Subsequent LC-MS analysis of chloroform extracts from *B. ambifaria* AMMD agar-grown cultures identified two, presumably isomeric, compounds with the same molecular formula as enacyloxin IIa. These compounds were purified by semipreparative HPLC. NMR spectroscopic analysis of the compounds identified them as enacyloxin IIa (Watanabe et al., 1992) and its novel Δ -4,5-*Z* stereoisomer, which we have named iso-enacyloxin IIa (Figure 3; Tables S2 and S3). LC-MS analyses of XAD-16 eluates from the mutants containing transposon insertions within the

gene mutants retained their normal anticandidal phenotype (Figure 1B).

Sequence Analysis of the Enacyloxin Biosynthetic Gene Cluster

Comparisons of the sequences of the proteins encoded by CDSs within the genomic island on chromosome 3 with proteins of known function identified 21 genes hypothesized to be involved in enacyloxin biosynthesis (Figure 2). Bamb_5925–5920 all encode proteins with similarity to so-called *cis*-AT modular PKSs, in which each module contains an AT domain for loading

Table 3. Activity of Purified Enacyloxin IIa and iso-Enacyloxin IIa on Bacteria and Yeast

Species and Strain	Minimal Inhibitory Concentration (mg/l)	
	Enacyloxin IIa	iso-Enacyloxin IIa
<i>B. multivorans</i> ATCC 17616	6.5	14
<i>B. dolosa</i> LMG 18943 ^T	7.5	15
<i>A. baumannii</i> OXA23 clone 2	3.0	7.0
<i>B. cenocepacia</i> J2315 (LMG 16656 ^T)	>100	>100
<i>P. aeruginosa</i> NCTC 12903	>100	>100
<i>C. albicans</i> SC5314	>100	>100

of the starter or extender unit onto the adjacent acyl carrier protein (ACP) domain (Figure 4A). Further analysis of each of these proteins using PKS and conserved domain search programs (Marchler-Bauer and Bryant, 2004; Yadav et al., 2003) showed that they constitute a loading module and nine chain-extension modules (Figure 4A).

The proposed structure of the intermediate assembled on the module 9 ACP domain (including the stereochemistry of the hydroxyl groups and the branching methyl group predicted using the method of Keatinge-Clay, 2007) (Figure S3) corresponds closely to the C-3 to C-23 portion of the polyketide chain of the proposed structure of enacyloxin IVa, a known intermediate in the biosynthesis of enacyloxin IIa in *Frateriura* sp. W-135 (Furukawa et al., 2007). The ACP-bound intermediate lacks the chloro groups attached to C-11 and C-18, the hydroxyl group attached to C-14, and the carbamoyl group attached to the C-19 hydroxyl group of enacyloxin IVa. These functional groups are proposed to be introduced by on-PKS or post-PKS tailoring reactions (vide supra). Δ -4,5 in the enacyloxin IVa polyketide chain is missing in the predicted structure of the intermediate attached to the module 9 ACP domain, because module 9 lacks the ketoreductase (KR) domain required to reduce the β -keto group to the corresponding hydroxyl group, which would be subsequently eliminated by the dehydratase (DH) domain to afford the double bond (Figure 4). Perhaps reduction of this keto group and subsequent elimination of water is catalyzed by the KR and DH domains within module 10 of the PKS. This might explain why a mixture of enacyloxin IIa isomers with Δ -4,5 geometries is produced by *B. ambifaria*. Interestingly, module 6 appears to be lacking a DH domain that would be expected to be required for introduction of Δ -10,11 into the intermediate attached to the ACP domain of module 10. Presumably, the dehydration reaction required to introduce this double bond is catalyzed by the module 7 DH domain. The final discrepancy between the predicted structure of the intermediate attached to the module 9 ACP domain and the proposed structure of enacyloxin IVa is between the absolute stereochemistry of C-15 proposed for enacyloxin IVa and the corresponding stereocenter in the intermediate (Figure 4). A recent “J-resolved HMBC-1” analysis of enacyloxin IVa (Furukawa et al., 2007) suggested that it has 15S absolute stereochemistry, whereas the corresponding stereocenter in

the intermediate is predicted on the basis of the hypothetical stereospecificity of the module 4 KR domain to have the 15R configuration (Keatinge-Clay, 2007). Further experiments will be needed to resolve this discrepancy.

An unusual feature of modules 2–5 and 7–9 is that they lack the AT domains invariably found within conventional *cis*-AT PKSs. No other genes within the cluster encode ATs, suggesting that the AT domain(s) within module 1 and/or module 6 catalyzes in *trans* loading of malonyl-CoA extender units onto the ACP domains within the AT-less PKS modules, as well as in *cis* loading of malonyl-CoA extender units onto the ACP domains within their own modules. Alternatively, loading of malonyl-CoA onto the ACP domains within the AT-less modules could be catalyzed by an acyltransferase encoded by a gene lying outside the enacyloxin biosynthetic gene cluster. A GCN5-related *N*-acetyltransferase (GNAT)-like domain within the loading module is hypothesized to catalyze decarboxylation of methylmalonyl-CoA and subsequent transfer of the resulting propionyl-CoA starter unit onto the adjacent ACP domain. Methylmalonyl-CoA is a novel substrate for GNAT domains within loading modules, which hitherto have only been reported to utilize malonyl-CoA (Gu et al., 2007).

Bamb_5919 encodes a protein that is similar to so-called *trans*-AT modular PKSs (Table 2), a group of proteins that is phylogenetically distinct from the *cis*-AT PKSs and in which the modules lack an AT domain for loading of the starter/extender unit onto the adjacent ACP domain, relying instead on separately encoded acyltransferases that load starter/extender units (usually malonyl-CoA) onto the ACP domains (Piel, 2010). Thus, the enacyloxin assembly line represents only the second example of a modular PKS that contains a mixture of proteins belonging to both the *cis*-AT and *trans*-AT phylogenetic groups (Piel, 2010). The other example is the kirromycin PKS, which consists mostly of proteins with similarity to *trans*-AT PKSs, but the last protein within the PKS portion of the assembly shows sequence similarity to *cis*-AT PKSs (Weber et al., 2008). Interestingly, kirromycin and enacyloxins have the same target—elongation factor Tu (EF-Tu) (Parmeggiani and Nissen, 2006). As expected for *trans*-AT PKSs, the protein encoded by Bamb_5919, which constitutes the last module of the enacyloxin PKS, lacks an AT domain (Figure 4). The lack of any genes encoding stand-alone ATs within the gene cluster suggests that the AT domain(s) within module 1 and/or module 6 of the enacyloxin PKS is responsible for loading malonyl-CoA onto the ACP domain within this protein. Alternatively, malonyl-CoA could be loaded onto the ACP domain by an AT encoded by a gene that lies outside the enacyloxin biosynthetic gene cluster. Four genes within the genome encoded AT domains with significant homology to Bamb_5925 and Bamb_5921; in order of decreasing homology these were Bamb_6476, Bamb_6235, Bamb_6222, and Bamb_0998. Only Bamb_6476 (an amino acid adenylation domain-containing protein; 15.37-fold up-regulation) and Bamb_0998 (a malonyl CoA-acyl carrier protein transacylase; 2.24-fold up-regulation) were expressed under enacyloxin-inducing conditions, but both at a level considerably below that of the pathway genes Bamb_5925 and Bamb_5921 (Table 2).

Release of the fully assembled polyketide chain from modular PKSs normally involves macrocyclization or hydrolysis catalyzed

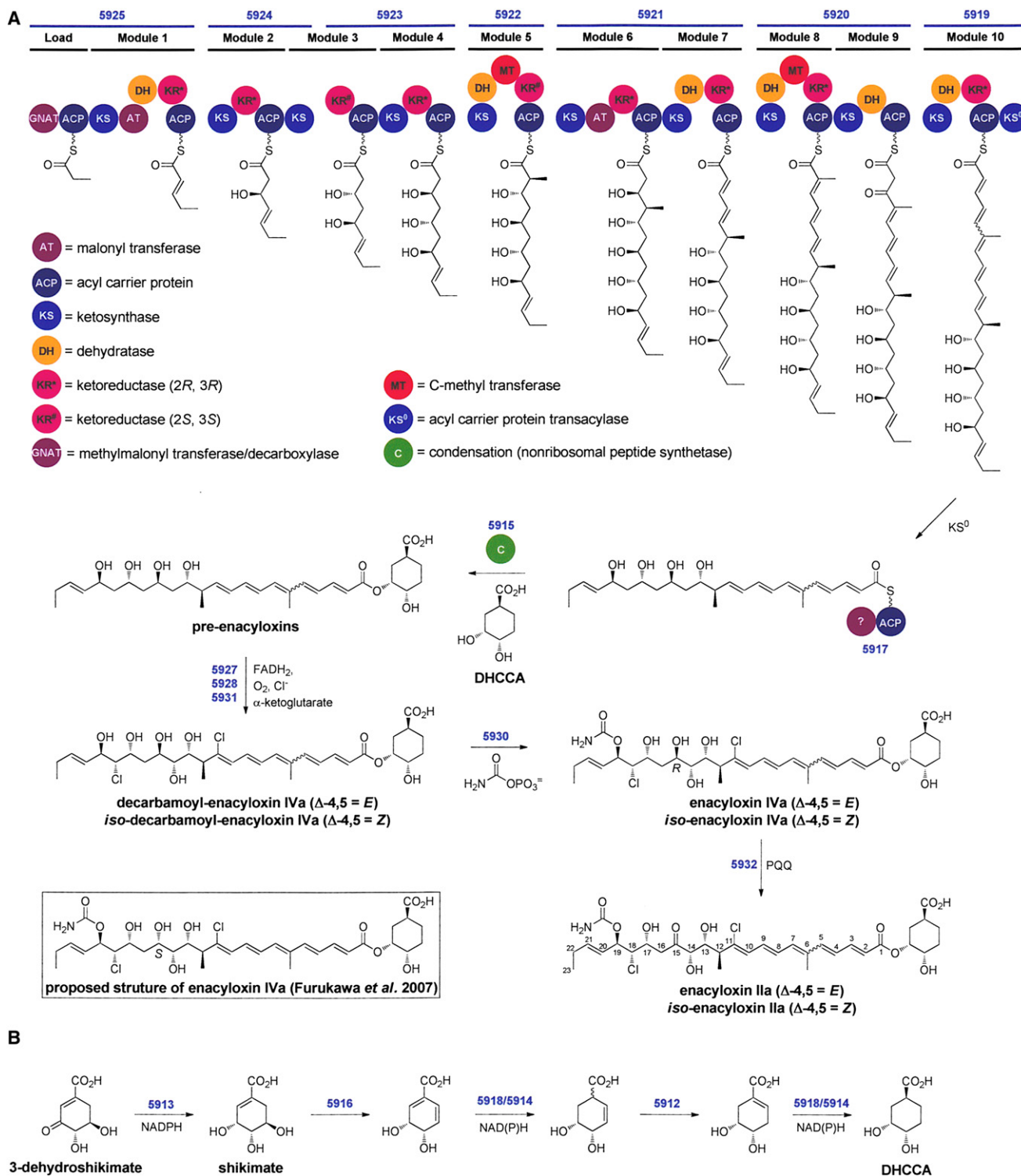


Figure 4. Proposed Pathway for Enacyloxin Biosynthesis

(A) Domain and module organization of the enacyloxin PKS, showing the proposed structures of chain-elongation intermediates after α and β carbon processing attached to the ACP domain in each module. The proposed mechanisms for condensation of the fully assembled polyketide chain with DHCCA and subsequent post-PKS tailoring reactions are shown. Note that the order of the tailoring reactions may be different from that shown and may occur during polyketide chain assembly rather than after. The structure for enacyloxin IVa proposed by Furukawa et al. (2007) on the basis of NMR experiments is shown in the box. The discrepancy in the absolute stereochemistry of C-15 between this structure and that predicted for enacyloxin IVa by the ketoreductase stereospecificity model of Keatinge-Clay (2007) is highlighted by stereochemical descriptors; an alignment of ketoreductase domains to support this stereospecificity is provided in Figure S3. (B) Proposed pathway for biosynthesis of DHCCA from 5-dehydroshikimate. *B. ambifaria* CDS numbers are shown in blue.

by a thioesterase domain at the C terminus of the last PKS module. The C-terminal domain within the last module of the enacyloxin PKS is a so-called ketosynthase^o (KS^o) domain (Figure 4). Such domains are common within *trans*-AT PKSs and are proposed to catalyze transacylation of intermediates in polyketide assembly from one ACP domain to another (Piel, 2010). We propose that the KS^o domain within module 10 of the enacyloxin PKS catalyzes transfer of the fully assembled polyketide chain from the module 10 ACP domain to an ACP domain within the protein encoded by Bamb_5917. Bamb_5915 encodes a protein that is similar to nonribosomal peptide synthetase condensation domains that is proposed to catalyze condensation of the C-3 hydroxyl group of (1S, 3R, 4S)-3,4-dihydroxycyclohexane carboxylic acid (DHCCA) with the thioester, to effect polyketide chain release via an unusual mechanism (König et al., 1997), forming pre-enacyloxins. DHCCA is proposed to be biosynthesized from shikimate, an intermediate in aromatic amino acid biosynthesis by the enzymes encoded by Bamb_5916, Bamb_5914, Bamb_5912, and Bamb_5918 (Figure 4). A putative shikimate dehydrogenase encoded by Bamb_5913 may boost the levels of shikimate for DHCCA biosynthesis by reduction of 5-dehydroshikimate.

The pre-enacyloxins are proposed to be converted to decarbamoyl-enacyloxin IVa and *iso*-decarbamoyl-enacyloxin IVa by the action of a putative FADH₂-, O₂-, and chloride-dependent halogenase (Blasiak and Drennan, 2009) which chlorinates C-11, a putative α -ketoglutarate-, O₂-, chloride-, and putative nonheme iron-dependent chlorinase (Blasiak and Drennan, 2009) which chlorinates C-18, and an α -ketoglutarate-, O₂-, and nonheme iron-dependent dioxygenase (Singh et al., 2008) which hydroxylates C-14, encoded by Bamb_5928, Bamb_5931, and Bamb_5927, respectively (Figure 4). Carbamoylation of decarbamoyl-enacyloxins IVa to give enacyloxin IVa and *iso*-enacyloxin IVa is likely catalyzed by the putative carbamoyl-transferase (Xu et al., 2002) encoded by Bamb_5930. The conversion of enacyloxin IVa to enacyloxin IIa in *Frateruia* sp. W-315 has been shown to be catalyzed by enacyloxin oxidase, an extracellular pyrroloquinoline quinone (PQQ)-dependent enzyme with an estimated molecular mass of 73 kDa (Oyama et al., 1994). Bamb_5932 encodes a putative 71.6 kDa PQQ-dependent enzyme that is proposed to catalyze the similar conversion of enacyloxins IVa to enacyloxins IIa in *B. ambifaria*.

Expression Analysis of *B. ambifaria* Genes Involved in Secondary Metabolite Biosynthesis

To map the genes that contribute to the biosynthesis of the enacyloxins on a global scale, a comparison of *B. ambifaria* AMMD gene expression after growth to stationary phase on glycerol (a carbon source inducing its production) versus glucose was performed using a custom microarray designed to the *B. ambifaria* AMMD genome. Over half the protein-encoding CDSs in *B. ambifaria* AMMD were significantly altered in expression (1.5-fold change, $p < 0.05$) by growth on glycerol (3405/6635; 51% of the genomic CDSs), with 2032 CDSs upregulated and 1373 CDSs downregulated (see Supplemental Information; ArrayExpress experiment accession number E-MEXP-2819). Nineteen of the 22 gene loci implicated in BAMB biosynthesis by transposon mutagenesis were significantly altered in expression (Table 2), corroborating the performance of the AMMD

custom microarray, a platform which has also been extensively validated on *B. cenocepacia* (Drevinek et al., 2008). Six gene clusters associated with the production of secondary metabolites were significantly upregulated, with the enacyloxin island and region encoding the AfcA lipopeptide (Kang et al., 1998) both having an atypical GC content indicative of acquisition by horizontal gene transfer (Table S4).

Genes within the enacyloxin biosynthesis island were among the most highly upregulated when *B. ambifaria* AMMD was grown to stationary phase on glycerol, with alterations ranging from 1.6- to 292-fold (Table S4). All the genes proposed to be involved in the biosynthesis of enacyloxin (Figures 2 and 4) were significantly upregulated, except for Bamb_5913, a putative shikimate dehydrogenase hypothesized to supply 5-dehydroshikimate for DHCCA biosynthesis (Figure 4; Table S4). The interconversion of shikimate and 3-dehydroshikimate is a step in the shikimate pathway for aromatic amino acid biosynthesis. Thus, Bamb_5913 appears to be redundant, which might explain why its expression is not upregulated under conditions that induce enacyloxin production. An efflux gene of the multidrug and toxin extrusion family (MATE), Bamb_5933, was also upregulated 102-fold, suggesting that it may provide the self-resistance pathway for enacyloxin. Both orphan LuxR regulators (Bamb_5910 and 5911) were also upregulated (Table S4), corroborating all the previous evidence showing that enacyloxin biosynthesis was under QS control.

Three other gene clusters correlating the biosynthesis of known Bcc antifungal antibiotics were also highly expressed (Table S4): the pyrrolnitrin biosynthetic gene cluster *prnA–D* (Bamb_4726–4729) (Schmidt et al., 2009), the 2-heptyl-3-hydroxy-4(1H)-quinolone (PQS)/4-hydroxy-3-methyl-2-alkylquinoline (HMAQ) biosynthetic gene cluster *hmqA–G* (Bamb_5763–5769) (Diggle et al., 2006; Vial et al., 2008), and a cluster of 26 genes (Bamb_6128–6153; only Bamb_6149 was not significantly upregulated) within which Bamb_6150 encoded a protein that was homologous to AfcA implicated in the biosynthesis of an antifungal lipopeptide from “*P. cepacia*” (Kang et al., 1998) (a Bcc isolate of unknown species). Both pyrrolnitrin (Figure S2) and the HMAQs (Figure S1) were detected in the Amberlite resin eluates from *B. ambifaria* AMMD, correlating the expression of these gene clusters to secondary metabolite secretion. The AFC lipopeptide appeared not to be present in these extracts. In addition, two further gene clusters, Bamb_3597–3617 and Bamb_6468–6482, predicted to direct the production of novel cryptic secondary metabolites, were also significantly overexpressed (Table S4).

DISCUSSION

B. ambifaria Enacyloxin Activity on MDR Pathogens and Other *Burkholderia*

We have demonstrated that Bcc bacteria can antagonize the growth of a range of clinically important pathogens associated with CF (Lipuma, 2010) and other multidrug-resistant infections (Coelho et al., 2006), in addition to their well-known antifungal biological control abilities in the natural environment (Parke and Gurian-Sherman, 2001). The ability of *B. ambifaria* to inhibit MDR Gram-negative bacteria such as *B. multivorans*, *B. dolosa*, and *A. baumannii* by secretion of enacyloxin IIa

and its novel isomer *iso*-enacyloxin is remarkable, especially as the susceptible *Burkholderia* species all belong to a taxonomically closely related complex (Coenye and Vandamme, 2003; Mahenthiralingam et al., 2005). Whereas antagonism toward fungi and Gram-positive bacteria has been observed in historical studies of either single isolates or limited collections of Bcc bacteria (Schmidt et al., 2009; Seyedsayamdost et al., 2010; Tawfik et al., 2010), the ability of *B. ambifaria* to inhibit the growth of closely related intrinsically antibiotic-resistant Bcc species is significant. The only other *Burkholderia* antimicrobial described that has significant activity on another *Burkholderia* species is the capistrain peptide of *B. thailandensis*, which is active on *B. caledonica* (Knappe et al., 2008).

Because a large proportion of Bcc isolates screened (Table 1) produced antimicrobial activity against *C. albicans* and *S. aureus*, which are also common CF pathogens (Lipuma, 2010), our laboratory-based observation lends weight to the hypothesis that infection with Bcc bacteria can reduce the polymicrobial content of sputum. *B. ambifaria* itself is not a common CF pathogen, reflecting less than 3% of all Bcc CF infections seen in the United States (Lipuma, 2010). However, it is a common environmental Bcc species (Coenye et al., 2001; Ramette et al., 2005). Two of the six enacyloxin-positive *B. ambifaria* isolates were recovered from infected CF patients, with the rest being of environmental origin. Given the limited number of CF infections caused by enacyloxin-positive *B. ambifaria* strains, determining whether the antibiotic is actually secreted during CF infection will not be straightforward. *B. cenocepacia*, which is the second most common Bcc CF infection (31% of cases; Lipuma, 2010), possesses significant anticandidal and anti-Gram-positive activity (Table 1). Thus, after identification of these antimicrobial metabolites, screening for their presence in CF sputum could be more readily performed.

Quorum Sensing and Accessory Loci Are Required for Enacyloxin Secretion

The quorum-sensing-regulated secretion of the enacyloxins by *B. ambifaria* is in agreement with the finding that multiple other *Burkholderia* antimicrobial secondary metabolites such as pyrrolnitrin (Schmidt et al., 2009), bactobolin (Seyedsayamdost et al., 2010), and thailandamide (Ishida et al., 2010) also require this form of cell-to-cell bacterial communication for their production. Although multiple LuxRI-type QS systems may occur in certain Bcc species such as *B. cenocepacia* (Malott et al., 2005), *B. ambifaria* AMMD only encodes the Bamb_4118 CepI synthase homolog and an adjacent CepR homolog (Bamb_4116) as the classical, putatively ancestral QS arrangement seen within the Bcc (Malott et al., 2005). The enacyloxin biosynthesis island encodes two LuxR-type orphan regulators, Bamb_5910 and Bamb_5911, which are upregulated by 4-fold (Table 2) and 11-fold (see Supplemental Information), respectively, during antibiotic secretion. Transposon mutation of Bamb_5910 (Table 2 and Figure 2) abolishes enacyloxin secretion; however, the insertion may have disrupted expression of both tandemly arranged *luxR* homologs. Therefore, although this mutant phenotype clearly links enacyloxin production to QS regulation, further work will be required to define how each *luxR* homolog functions to modulate *B. ambifaria* gene expression. Both QS regulator genes reside within the enacyloxin

biosynthesis genomic island, illustrating the unique capacity for *Burkholderia* bacteria to acquire, regulate, and express large, complex foreign gene clusters. In addition to its QS requirement, enacyloxin production is also carbon source dependent, suggesting further complexity in antibiotic regulation. Overall, these findings suggest that future screening of *Burkholderia* species for antimicrobial secondary metabolites should take into account both metabolic factors and regulatory systems such as QS dependency.

Although the enacyloxin biosynthesis island appeared to be relatively self-contained encoding the biosynthetic enzymes (e.g., PKS modules Bamb_5919–5952) as well as regulators (e.g., LuxR-type regulators Bamb_5910 and Bamb_5911) and putative self-resistance proteins (e.g., the MATE efflux protein Bamb_5933), the mutagenesis and global gene expression data also implicated multiple accessory loci in enacyloxin secretion. In the context of novel biological functions being linked to microbial genes, one of the most intriguing genes identified was the hypothetical gene Bamb_5367, which is located on an RHS-genetic locus of chromosome 2. Five independent transposon mutations mapped to Bamb_5367, suggesting this region was integral to enacyloxin secretion (Table 2). RHS loci have been linked to type VI secretion systems, and recent bioinformatic analyses of these VGR proteins indicate that they may evolve function by acquisition and switching of alternate C-terminal sequences or tips (Jackson et al., 2009). Our data suggest that there is a novel link to enacyloxin export for this *B. ambifaria* RHS-VGR locus. Although all the transposon mutations in this region mapped to Bamb_5367, significant upregulation of this gene was not detected (Table 2). However, both Bamb_5366 and Bamb_5368 were significantly upregulated during enacyloxin biosynthesis (2.3- and 1.7-fold, respectively; see Supplemental Information), corroborating the involvement of the RHS locus in antibiotic export and suggesting that Bamb_5368 may act as an alternative C terminus for Bamb_5366. The high GC content of the PKS genes (Bamb_5919 to 5925 had a mean GC content of 74.5%; Table S4) within the enacyloxin biosynthesis island suggests the cluster may have originated in an actinomycete. The novel involvement of RHS loci in enacyloxin secretion suggests that after acquisition of the biosynthesis island, *B. ambifaria* had to tailor antibiotic secretion to suite its Gram-negative physiology, illustrating the versatility of *Burkholderia* in assembling and expressing complex metabolic pathways (Chain et al., 2006).

Enacyloxin Biosynthesis and Its Manipulation to Produce Novel Antibiotics

To date, enacyloxins have only been reported to be produced by a single bacterial isolate, *Frateriia* sp. W-315, a Gammaproteobacterium of the family Xanthomonadaceae (Furukawa et al., 2007). Apart from the PQQ-dependent oxidation reaction that converts enacyloxin IVa to enacyloxin IIa (Oyama et al., 1994), nothing is known about enacyloxin biosynthesis in *Frateriia*. The discovery of enacyloxin IIa and its novel stereoisomer *iso*-enacyloxin IIa as the metabolic products of a cryptic modular polyketide synthase biosynthetic gene cluster in *B. ambifaria* has allowed a plausible pathway for enacyloxin biosynthesis to be proposed. This hypothetical pathway involves several unusual or unique features, including only the second example of a hybrid

PKS consisting of proteins with sequence similarity to both *cis*-AT and *trans*-AT variants, novel methylmalonyl-CoA specificity for a GNAT-like domain within a PKS loading module, condensation domain-mediated polyketide chain release via *intermolecular* ester bond formation, a novel route for DHCCA biosynthesis from shikimate, regiospecific chlorination of a polyene catalyzed by a flavin-dependent chlorinase (only aromatic rings have been reported to be chlorinated by such enzymes to date), and *stereospecific* hydrocarbon chlorination by a nonheme iron- and α -ketoglutarate-dependent chlorinase. Remarkably, only two of the nine PKS chain-extension modules with sequence similarity to *cis*-AT proteins appear to contain AT domains, and no stand-alone ATs are encoded by genes within the enacyloxin biosynthetic gene cluster. This suggests that the ACP domains within the seven PKS modules that are similar to *cis*-AT proteins, but lack AT domains, are loaded with malonyl extender units either by the two modules containing AT domains or by an AT encoded by a gene lying outside the enacyloxin biosynthetic gene cluster (although no candidate for this additional AT was identified in the transposon mutagenesis experiments, and homology searches only revealed two candidate AT-containing genes expressed under enacyloxin-inducing conditions).

The antibacterial activity of enacyloxins stems from their ability to inhibit protein synthesis by binding to EF-Tu, which locks the protein in the GTP-bound conformation (regardless of whether GTP or GDP is bound), preventing release of aminoacyl-tRNA after delivery to the acceptor site of the ribosome (Parmeggiani et al., 2006). Interestingly, the expression of multiple ribosomal and regulatory RNAs is upregulated during enacyloxin biosynthesis (see Supplemental Information), suggesting that their overproduction may contribute to the enacyloxin resistance in *B. ambifaria*. The X-ray crystal structure of enacyloxin IIa bound to a complex of EF-Tu with a nonhydrolyzable GTP analog pinpoints important functional groups in the antibiotic that interact with the elongation factor. This information coupled with the proposed pathway for enacyloxin biosynthesis should stimulate future biosynthetic engineering efforts to produce novel enacyloxin analogs with potential applications in the treatment of MDR Gram-negative infections.

SIGNIFICANCE

Gram-negative *B. cepacia* complex bacteria are known for their ability to secrete a range of antifungal secondary metabolites that contribute to their biopesticidal phenotype. Bcc bacteria also cause human opportunistic infections in individuals with CF. However, it is not known whether they can antagonize the growth of other pathogens which infect the lungs of these individuals. Recent revisions in Bcc taxonomy and our curiosity about the ability of Bcc bacteria to compete with other CF pathogens stimulated us to perform a systematic survey of Bcc antimicrobial secretion. Of 268 representative Bcc isolates screened, 85 were antifungal, 64 were anti-Gram positive, and 6 *B. ambifaria* isolates inhibited a range of multidrug-resistant (MDR) Gram-negative bacteria including the CF pathogen *B. multivorans*. Using transposon mutagenesis and global gene expression analysis, production of the *B. ambifaria*

antibacterial was mapped to a cluster of cryptic, quorum-sensing-regulated genes within the genome of *B. ambifaria* strain AMMD, several of which encode proteins that are similar to modular polyketide synthases (PKSs). Isolation and structure elucidation demonstrated that the antibiotic was a mixture of enacyloxin IIa, an unusual polyene targeting elongation factor Tu, and a stereoisomer we designated *iso-enacyloxin IIa*. Sequence analysis of the proteins encoded within the enacyloxin biosynthetic gene cluster allowed a complete hypothetical pathway for enacyloxin biosynthesis to be proposed. This pathway involves several distinctive features including a very unusual hybrid *cis*-acyltransferase (*cis*-AT)/*trans*-AT PKS consisting of a loading module containing a GCN5-related *N*-acetyltransferase domain that appears to be specific for methylmalonyl-CoA, nine chain-extension modules with sequence similarity to *cis*-AT PKSs (seven of which lack AT domains), and a single AT-less chain-extension module with sequence similarity to *trans*-AT PKSs. These findings suggest that the Bcc may be an underexploited resource for the discovery of antibiotics with distinctive biosynthetic pathways and potent activity against MDR pathogens.

EXPERIMENTAL PROCEDURES

Strains and Culture Conditions

All *Burkholderia* isolates were drawn from previous studies (Mahenthiralingam et al., 2008) and had been accurately identified to the species level by either MLST (Baldwin et al., 2005) or *recA* sequence analysis (Payne et al., 2005). Genome-sequenced Bcc strains used were as follows: *B. lata* 383, *B. multivorans* ATCC 17616, *B. ambifaria* AMMD, *B. ambifaria* MC40-6, *B. vietnamiensis* G4, *B. cenocepacia* J2315, *B. cenocepacia* HI2424, *B. cenocepacia* AU1054, and *B. cenocepacia* IIB MC0-3, with sequence data available at the *Burkholderia* Genome Database (<http://www.burkholderia.com>), and *B. contaminans* LMG 23255, for which the *Burkholderia* SAR-1 metagenome serves as a reference sequence (Mahenthiralingam et al., 2006). Other representative Bcc isolates examined were *B. cepacia* ATCC 25416^T, *B. dolosa* LMG 18943, *B. cenocepacia* BCC0524, *B. cenocepacia* IIAA, *B. cenocepacia* BCC0048, *B. stabiliz* LMG 18888, *B. cenocepacia* CZ1238, *B. cenocepacia* BCC1434, and *B. cenocepacia* BCC1436. The growth of *Burkholderia* (at 30°C) was carried out on tryptic soya medium, whereas production of antibiotics was performed on a minimal salts medium with 4 g/l glycerol as the carbon source (BSM-G; O'Sullivan et al., 2007). Antibiotic susceptibility testing was carried out using a standardized broth microdilution assay (Rose et al., 2009) with a maximum concentration of 100 mg/l enacyloxin tested.

Antimicrobial Activity Screens

A classical overlay assay was used to screen for antimicrobial activity (see Supplemental Information). Briefly, each Bcc strain was grown as a single colony on BSM-G agar, killed with chloroform vapor after growth, and overlaid with soft Isosensitest agar (Oxoid) seeded with a susceptibility-testing reference species. Antimicrobial activity was scored by measuring the zone of clearing (mm) around the Bcc colony; in the initial screen of the Bcc collection isolates, those producing a zone of clearing greater than 10 mm were scored as positive for antimicrobial activity (Table 1).

Transposon Mutagenesis and Genome Mapping

B. ambifaria strain AMMD was subjected to transposon mutagenesis with mini-Tn5-Km2 as described (O'Sullivan et al., 2007) and a bank of 1920 mutants was created. Mutants were screened for reduction, loss of, and increased activity against *B. multivorans* ATCC 17616 using the overlay assay. The loci flanking the transposon insertions were sequenced (O'Sullivan et al., 2007) and correlated to the *B. ambifaria* AMMD genome using the web database <http://www.burkholderia.com>.

PCR of PKS Genes

PCR primers were designed to amplify the *B. ambifaria* AMMD PKS genes Bamb_5925, Bamb_5921, and Bamb_5919 (see Supplemental Information). A standard PCR amplification was performed on BAMM-positive *B. ambifaria* strains, and amplification products were subjected to DNA sequence analysis to corroborate their identity as previously described (Payne et al., 2005).

Global Gene Expression Analysis

Custom gene expression microarrays based on Agilent 60-mer SurePrint technology were designed to the genome sequence of *B. ambifaria* strain AMMD by Oxford Gene Technology (ArrayExpress [http://www.ebi.ac.uk/arrayexpress] design number A-MEXP-1839). *B. ambifaria* AMMD gene expression induced by growth on glycerol was compared to that on glucose as previously described (Drevinek et al., 2008) (see Supplemental Information) with three replicate experiments performed. Arrays were scanned and processed for bioinformatic analysis using GeneSpring GX version 7.3.1 as described (Drevinek et al., 2008), and the experiment was submitted to ArrayExpress (accession number E-MEXP-2819). Genes which altered expression by greater than 1.5-fold ($p < 0.05$) after growth on glycerol were identified (see Supplemental Information).

Antibiotic Isolation, Structure Elucidation, and Detection

Antibiotics were isolated by adsorption onto an Amberlite XAD-16 neutral crosslinked polystyrene resin (Ribeiro and Ribeiro, 2003) and subsequently eluted with methanol (see Supplemental Information). Semipreparative HPLC was used to purify antibiotics, and fractions were analyzed by HR-MS. The structures of the products of the cryptic PKS cluster were elucidated using a combination of HR-MS, MS/MS, and NMR experiments as described (see Supplemental Information). All formulas generated from the parent ion and fragment ions are consistent with the molecular formula of enacyloxin IIa (Figures 3 and 4). LC-MS analyses were applied to the XAD-16 eluates of AMMD and transposon mutants (Bamb_5925 and Bamb_5919; Figure 1) to correlate mutation of the PKS cluster with abrogation of enacyloxin biosynthesis (see Supplemental Information).

ACCESSION NUMBERS

The custom *B. ambifaria* AMMD microarray design has been submitted to ArrayExpress (http://www.ebi.ac.uk/arrayexpress) under design number A-MEXP-1839. The microarray data for the experiment comparing *B. ambifaria* AMMD gene expression under antibiotic-inducing and -noninducing growth conditions have been submitted to ArrayExpress under experiment accession number E-MEXP-2819.

SUPPLEMENTAL INFORMATION

Supplemental Information includes three figures, four tables, and Supplemental Experimental Procedures and can be found with this article online at doi:10.1016/j.chembiol.2011.01.020.

ACKNOWLEDGMENTS

E.M. thanks Haizun Abd Ghani, Aled Roberts, and Laura Evans for technical assistance. The development and application of the custom *B. ambifaria* AMMD microarray was funded by the U.S. Cystic Fibrosis Therapeutics Burkholderia array program (grant MAHENT06V0). The Bruker MaXis mass spectrophotometer used in this research was obtained through Birmingham Science City: Innovative Uses for Advanced Materials in the Modern World (West Midlands Centre for Advanced Materials Project 2), with support from Advantage West Midlands and part funded by the European Regional Development Fund.

Received: December 7, 2010

Revised: January 24, 2011

Accepted: January 26, 2011

Published: May 26, 2011

REFERENCES

- Baldwin, A., Mahenthalingam, E., Thickett, K.M., Honeybourne, D., Maiden, M.C., Govan, J.R., Speert, D.P., Lipuma, J.J., Vandamme, P., and Dowson, C.G. (2005). Multilocus sequence typing scheme that provides both species and strain differentiation for the *Burkholderia cepacia* complex. *J. Clin. Microbiol.* **43**, 4665–4673.
- Blasiak, L.C., and Drennan, C.L. (2009). Structural perspective on enzymatic halogenation. *Acc. Chem. Res.* **42**, 147–155.
- Chain, P.S., Deneff, V.J., Konstantinidis, K.T., Vergez, L.M., Agullo, L., Reyes, V.L., Hauser, L., Cordova, M., Gomez, L., Gonzalez, M., et al. (2006). *Burkholderia xenovorans* LB400 harbors a multi-replicon, 9.73-Mbp genome shaped for versatility. *Proc. Natl. Acad. Sci. USA* **103**, 15280–15287.
- Chernish, R.N., and Aaron, S.D. (2003). Approach to resistant Gram-negative bacterial pulmonary infections in patients with cystic fibrosis. *Curr. Opin. Pulm. Med.* **9**, 509–515.
- Coelho, J.M., Turton, J.F., Kaufmann, M.E., Glover, J., Woodford, N., Warner, M., Palepou, M.F., Pike, R., Pitt, T.L., Patel, B.C., et al. (2006). Occurrence of carbapenem-resistant *Acinetobacter baumannii* clones at multiple hospitals in London and Southeast England. *J. Clin. Microbiol.* **44**, 3623–3627.
- Coenye, T., and Vandamme, P. (2003). Diversity and significance of *Burkholderia* species occupying diverse ecological niches. *Environ. Microbiol.* **5**, 719–729.
- Coenye, T., Mahenthalingam, E., Henry, D., LiPuma, J.J., Laevens, S., Gillis, M., Speert, D.P., and Vandamme, P. (2001). *Burkholderia ambifaria* sp. nov., a novel member of the *Burkholderia cepacia* complex including biocontrol and cystic fibrosis-related isolates. *Int. J. Syst. Evol. Microbiol.* **51**, 1481–1490.
- Diggle, S.P., Lumjiaktase, P., Dipilato, F., Winzer, K., Kunakorn, M., Barrett, D.A., Chhabra, S.R., Camara, M., and Williams, P. (2006). Functional genetic analysis reveals a 2-alkyl-4-quinolone signaling system in the human pathogen *Burkholderia pseudomallei* and related bacteria. *Chem. Biol.* **13**, 701–710.
- Drevinek, P., Holden, M.T., Ge, Z., Jones, A.M., Ketchell, I., Gill, R.T., and Mahenthalingam, E. (2008). Gene expression changes linked to antimicrobial resistance, oxidative stress, iron depletion and retained motility are observed when *Burkholderia cenocepacia* grows in cystic fibrosis sputum. *BMC Infect. Dis.* **8**, 121.
- Furukawa, H., Kiyota, H., Yamada, T., Yaosaka, M., Takeuchi, R., Watanabe, T., and Kuwahara, S. (2007). Stereochemistry of enacyloxins part 4. Complete structural and configurational assignment of the enacyloxin family, a series of antibiotics from *Frateuria* sp. W-315. *Chem. Biodivers.* **4**, 1601–1604.
- Gu, L., Geders, T.W., Wang, B., Gerwick, W.H., Hakansson, K., Smith, J.L., and Sherman, D.H. (2007). GNAT-like strategy for polyketide chain initiation. *Science* **318**, 970–974.
- Ishida, K., Lincke, T., Behnken, S., and Hertweck, C. (2010). Induced biosynthesis of cryptic polyketide metabolites in a *Burkholderia thailandensis* quorum sensing mutant. *J. Am. Chem. Soc.* **132**, 13966–13968.
- Jackson, A.P., Thomas, G.H., Parkhill, J., and Thomson, N.R. (2009). Evolutionary diversification of an ancient gene family (rhs) through C-terminal displacement. *BMC Genomics* **10**, 584.
- Kalish, L.A., Waltz, D.A., Dovey, M., Potter-Bynoe, G., McAdam, A.J., Lipuma, J.J., Gerard, C., and Goldmann, D. (2006). Impact of *Burkholderia dolosa* on lung function and survival in cystic fibrosis. *Am. J. Respir. Crit. Care Med.* **173**, 421–425.
- Kang, Y., Carlson, R., Tharpe, W., and Schell, M.A. (1998). Characterization of genes involved in biosynthesis of a novel antibiotic from *Burkholderia cepacia* BC11 and their role in biological control of *Rhizoctonia solani*. *Appl. Environ. Microbiol.* **64**, 3939–3947.
- Keatinge-Clay, A.T. (2007). A tylosin ketoreductase reveals how chirality is determined in polyketides. *Chem. Biol.* **14**, 898–908.
- Keum, Y.S., Lee, Y.J., Lee, Y.H., and Kim, J.H. (2009). Effects of nutrients on quorum signals and secondary metabolite productions of *Burkholderia* sp. O33. *J. Microbiol. Biotechnol.* **19**, 1142–1149.

- Knappe, T.A., Linne, U., Zirah, S., Rebuffat, S., Xie, X., and Marahiel, M.A. (2008). Isolation and structural characterization of capistrin, a lasso peptide predicted from the genome sequence of *Burkholderia thailandensis* E264. *J. Am. Chem. Soc.* **130**, 11446–11454.
- König, A., Schwecke, T., Molnar, I., Bohm, G.A., Lowden, P.A.S., Staunton, J., and Leadlay, P.F. (1997). The pipecolate-incorporating enzyme for the biosynthesis of the immunosuppressant rapamycin—nucleotide sequence analysis, disruption and heterologous expression of rapP from *Streptomyces hygroscopicus*. *Eur. J. Biochem.* **247**, 526–534.
- Lipuma, J.J. (2010). The changing microbial epidemiology in cystic fibrosis. *Clin. Microbiol. Rev.* **23**, 299–323.
- Mahenthalingam, E., Urban, T.A., and Goldberg, J.B. (2005). The multifarious, multireplicon *Burkholderia cepacia* complex. *Nat. Rev. Microbiol.* **3**, 144–156.
- Mahenthalingam, E., Baldwin, A., Drevinek, P., Vanlaere, E., Vandamme, P., LiPuma, J.J., and Dowson, C.G. (2006). Multilocus sequence typing breathes life into a microbial metagenome. *PLoS One* **1**, e17.
- Mahenthalingam, E., Baldwin, A., and Dowson, C.G. (2008). *Burkholderia cepacia* complex bacteria: opportunistic pathogens with important natural biology. *J. Appl. Microbiol.* **104**, 1539–1551.
- Malott, R.J., Baldwin, A., Mahenthalingam, E., and Sokol, P.A. (2005). Characterization of the cciIR quorum-sensing system in *Burkholderia cenocepacia*. *Infect. Immun.* **73**, 4982–4992.
- Marchler-Bauer, A., and Bryant, S.H. (2004). CD-Search: protein domain annotations on the fly. *Nucleic Acids Res.* **32**, W327–W331.
- Moon, S.-S., Kang, P.M., Park, K.S., and Kim, C.H. (1996). Plant growth promoting and fungicidal 4-quinolones from *Pseudomonas cepacia*. *Phytochemistry* **42**, 365–368.
- Nguyen, T., Ishida, K., Jenke-Kodama, H., Dittmann, E., Gurgui, C., Hochmuth, T., Taudien, S., Platzer, M., Hertweck, C., and Piel, J. (2008). Exploiting the mosaic structure of *trans*-acyltransferase polyketide synthases for natural product discovery and pathway dissection. *Nat. Biotechnol.* **26**, 225–233.
- O'Sullivan, L.A., Weightman, A.J., Jones, T.H., Marchbank, A.M., Tiedje, J.M., and Mahenthalingam, E. (2007). Identifying the genetic basis of ecologically and biotechnologically useful functions of the bacterium *Burkholderia vietnamiensis*. *Environ. Microbiol.* **9**, 1017–1034.
- Oyama, R., Watanabe, T., Hanzawa, H., Sano, T., Sugiyama, T., and Izaki, K. (1994). An extracellular quinoprotein oxidase that catalyzes conversion of enacyloxin IVa to enacyloxin IIa. *Biosci. Biotechnol. Biochem.* **58**, 1914–1917.
- Parke, J.L., and Gurian-Sherman, D. (2001). Diversity of the *Burkholderia cepacia* complex and implications for risk assessment of biological control strains. *Annu. Rev. Phytopathol.* **39**, 225–258.
- Parmeggiani, A., and Nissen, P. (2006). Elongation factor Tu-targeted antibiotics: four different structures, two mechanisms of action. *FEBS Lett.* **580**, 4576–4581.
- Parmeggiani, A., Krab, I.M., Watanabe, T., Nielsen, R.C., Dahlberg, C., Nyborg, J., and Nissen, P. (2006). Enacyloxin IIa pinpoints a binding pocket of elongation factor Tu for development of novel antibiotics. *J. Biol. Chem.* **281**, 2893–2900.
- Partida-Martinez, L.P., and Hertweck, C. (2007). A gene cluster encoding rhizoxin biosynthesis in “*Burkholderia rhizoxina*”, the bacterial endosymbiont of the fungus *Rhizopus microsporus*. *ChemBioChem* **8**, 41–45.
- Payne, G.W., Vandamme, P., Morgan, S.H., LiPuma, J.J., Coenye, T., Weightman, A.J., Jones, T.H., and Mahenthalingam, E. (2005). Development of a recA gene-based identification approach for the entire *Burkholderia* genus. *Appl. Environ. Microbiol.* **71**, 3917–3927.
- Piel, J. (2010). Biosynthesis of polyketides by *trans*-AT polyketide synthases. *Nat. Prod. Rep.* **27**, 996–1047.
- Ramette, A., Lipuma, J.J., and Tiedje, J.M. (2005). Species abundance and diversity of *Burkholderia cepacia* complex in the environment. *Appl. Environ. Microbiol.* **71**, 1193–1201.
- Ribeiro, M.H., and Ribeiro, I.A. (2003). Modelling the adsorption kinetics of erythromycin onto neutral and anionic resins. *Bioprocess Biosyst. Eng.* **26**, 49–55.
- Rohm, B., Scherlach, K., and Hertweck, C. (2010). Biosynthesis of the mitochondrial adenine nucleotide translocase (ATPase) inhibitor bongkreic acid in *Burkholderia gladioli*. *Org. Biomol. Chem.* **8**, 1520–1522.
- Rose, H., Baldwin, A., Dowson, C.G., and Mahenthalingam, E. (2009). Biocide susceptibility of the *Burkholderia cepacia* complex. *J. Antimicrob. Chemother.* **63**, 502–510.
- Schmidt, S., Blom, J.F., Perntaler, J., Berg, G., Baldwin, A., Mahenthalingam, E., and Eberl, L. (2009). Production of the antifungal compound pyrrolnitrin is quorum sensing-regulated in members of the *Burkholderia cepacia* complex. *Environ. Microbiol.* **11**, 1422–1437.
- Seyedsayamdost, M.R., Chandler, J.R., Blodgett, J.A., Lima, P.S., Duerkop, B.A., Oinuma, K., Greenberg, E.P., and Clardy, J. (2010). Quorum-sensing-regulated bacterolin production by *Burkholderia thailandensis* E264. *Org. Lett.* **12**, 716–719.
- Singh, G.M., Fortin, P.D., Koglin, A., and Walsh, C.T. (2008). β -hydroxylation of the aspartyl residue in the phytotoxin syringomycin E: characterization of two candidate hydroxylases AspH and SyrP in *Pseudomonas syringae*. *Biochemistry* **47**, 11310–11320.
- Tawfik, K.A., Jeffs, P., Bray, B., Dubay, G., Falkinham, J.O., Mesbah, M., Youssef, D., Khalifa, S., and Schmidt, E.W. (2010). Burkholdines 1097 and 1229, potent antifungal peptides from *Burkholderia ambifaria* 2.2N. *Org. Lett.* **12**, 664–666.
- Vanlaere, E., Baldwin, A., Gevers, D., Henry, D., De Brandt, E., LiPuma, J.J., Mahenthalingam, E., Speert, D.P., Dowson, C., and Vandamme, P. (2009). Taxon K, a complex within the *Burkholderia cepacia* complex, comprises at least two novel species, *Burkholderia contaminans* sp. nov. and *Burkholderia lata* sp. nov. *Int. J. Syst. Evol. Microbiol.* **59**, 102–111.
- Vial, L., Groleau, M.C., Dekimpe, V., and Deziel, E. (2007). *Burkholderia* diversity and versatility: an inventory of the extracellular products. *J. Microbiol. Biotechnol.* **17**, 1407–1429.
- Vial, L., Lepine, F., Milot, S., Groleau, M.C., Dekimpe, V., Woods, D.E., and Deziel, E. (2008). *Burkholderia pseudomallei*, *B. thailandensis*, and *B. ambifaria* produce 4-hydroxy-2-alkylquinoline analogues with a methyl group at the 3 position that is required for quorum-sensing regulation. *J. Bacteriol.* **190**, 5339–5352.
- Watanabe, T., Izaki, K., and Takahashi, H. (1982). New polyenic antibiotics active against Gram-positive and -negative bacteria. I. Isolation and purification of antibiotics produced by *Gluconobacter* sp. W-315. *J. Antibiot. (Tokyo)* **35**, 1141–1147.
- Watanabe, T., Sugiyama, T., Takahashi, M., Shima, J., Yamashita, K., Izaki, K., Furihata, K., and Seto, H. (1992). New polyenic antibiotics active against Gram-positive and Gram-negative bacteria IV. Structural elucidation of enacyloxin IIa. *J. Antibiot. (Tokyo)* **45**, 470–475.
- Weber, T., Laiple, K.J., Pross, E.K., Textor, A., Grond, S., Welzel, K., Pelzer, S., Vente, A., and Wohlleben, W. (2008). Molecular analysis of the kirromycin biosynthetic gene cluster revealed β -alanine as precursor of the pyridone moiety. *Chem. Biol.* **15**, 175–188.
- Xu, H., Wang, Z.-X., Schmidt, J., Heide, L., and Li, S.-M. (2002). Genetic analysis of the biosynthesis of the pyrrole and carbamoyl moieties of coumermycin A1 and novobiocin. *Mol. Genet. Genomics* **268**, 387–396.
- Yadav, G., Gokhale, R.S., and Mohanty, D. (2003). SEARCHPKS: a program for detection and analysis of polyketide synthase domains. *Nucleic Acids Res.* **31**, 3654–3658.
- Zerikly, M., and Challis, G.L. (2009). Strategies for the discovery of new natural products by genome mining. *ChemBioChem* **10**, 625–633.